

Highly Selective Monomethylation of Amines with CO₂/H₂ via Ag/Al₂O₃ as a Catalyst

Yan Long^{+, [a]}, Jie He^{+, [a]}, Hang Zhang,^[b] Yingkang Chen,^[b] Kang Liu,^[b] Junwei Fu,^[b] Hongmei Li,^[b, d] Li Zhu,^[b] Zhang Lin,^[c] Andrei Stefanu,^[e] Emiliano Cortes,^{*, [e]} Mingshan Zhu,^{*, [a]} and Min Liu^{*, [b]}

Abstract: The selective synthesis of monomethylated amines with CO₂ is particularly challenging because the formation of tertiary amines is thermodynamically more favorable. Herein, a new strategy for the controllable synthesis of N-monomethylated amines from primary amines and CO₂/H₂ is explored. First-principle calculations reveal that the dissociation of H₂ via an heterolytic route reduces the reactivity of methylated amines and thus inhibit successive methylation. In situ DRIFTS proves the process of formation and decomposition of

ammonium salt by secondary amine reversible binding with H⁺ on the Ag/Al₂O₃ catalyst, thereby reducing its reactivity. Meanwhile, the energy barrier for the rate-determining step of monomethylation was much lower than that of overmethylation (0.34 eV vs. 0.58 eV) means amines monomethylation in preference to successive methylation. Under optimal reaction conditions, a variety of amines were converted to the corresponding monomethylated amines in good to excellent yields, and more than 90% yield of product was obtained.

Introduction

The rapid increase in CO₂ emission is already leading to severe environmental issues, such as global warming and ocean

acidification. Many strategies were proposed to control and/or mitigate CO₂ emission, such as direct removal of CO₂ from the air by solvents and solid sorbents,^[1] convert CO₂ to chemicals^[2] and so on. Among these, catalytic conversion of CO₂ has attracted a lot of attention. The transformation of CO₂ into CO,^[3] HCOOH,^[4] CH₄,^[5] CH₃OH^[6] or fuels^[7] has been extensively studied. In addition, using CO₂ as C1 source in the synthesis of many chemicals also constitutes an alternative promising direction.^[8] Among the various organic synthesis that could use CO₂ as reactant, N-methylation of amines is one of the most important transformations due to their wide range of applications and large scale industrial production.^[9] Traditionally, toxic reagents are employed in the synthesis of methylated amines, such as methyl iodide,^[10] formaldehyde,^[11] dimethyl sulfoxide (DMSO),^[12] among others. These synthesis routes are linked to a series of post-processing issues with obvious environmental consequences. Recently, greener methylation reagents including CH₃OH,^[13] HCOOH,^[14] dimethyl carbonate (DMC)^[15] and CO₂^[16] have been proposed and tested. From the perspective of green and economic chemistry, using CO₂ as a N-methylation reagent is undoubtedly a very attractive route, because CO₂ is a cheap, non-toxic and highly abundant gas. The N-monomethylated amines as one particular kind of N-methylamines are widely used in the synthesis of medicines, pesticides and dyes.^[11] However, there is still a great challenge for selective monomethylation of amines by using CO₂ as C1 source, due to the higher reactivity of secondary amines compared to primary amines. As such, N-monomethylamine is prone to over-methylation, generating tertiary amines, which destroy the selectivity of the target product.^[17]

Beller's and Cantat's groups firstly employed CO₂ and amines to synthesize methylated amines using Zn–N-heterocyclic carbene complexes and Ru-phosphine complexes as catalysts, respectively.^[16d, f] Following, a plethora of homoge-

[a] Dr. Y. Long,⁺ J. He,⁺ Prof. M. Zhu
Guangdong Key Laboratory of Environmental Pollution and Health
School of Environment, Jinan University
511443 Guangzhou (P. R. China)
E-mail: zhulingshan@jnu.edu.cn

[b] H. Zhang, Y. Chen, K. Liu, J. Fu, H. Li, L. Zhu, Prof. M. Liu
Hunan Joint International Research Center for Carbon Dioxide Resource Utilization
State Key Laboratory of Powder Metallurgy, School of Physical and Electronics
Central South University
410083 Changsha (P. R. China)
E-mail: minliu@csu.edu.cn

[c] Z. Lin
Chinese National Engineering Research Centre for Control & Treatment of Heavy Metal Pollution, School of Metallurgy and Environment
Central South University
410083 Changsha (China)

[d] H. Li
School of Materials Science and Engineering, Zhengzhou University
450002 Zhengzhou (P. R. China)

[e] A. Stefanu, Prof. E. Cortes
Nanoinstitut München, Fakultät für Physik
Ludwig-Maximilians-Universität München
80539 München, Germany
E-mail: Emiliano.Cortes@lmu.de

[*] These authors contributed equally to this work.

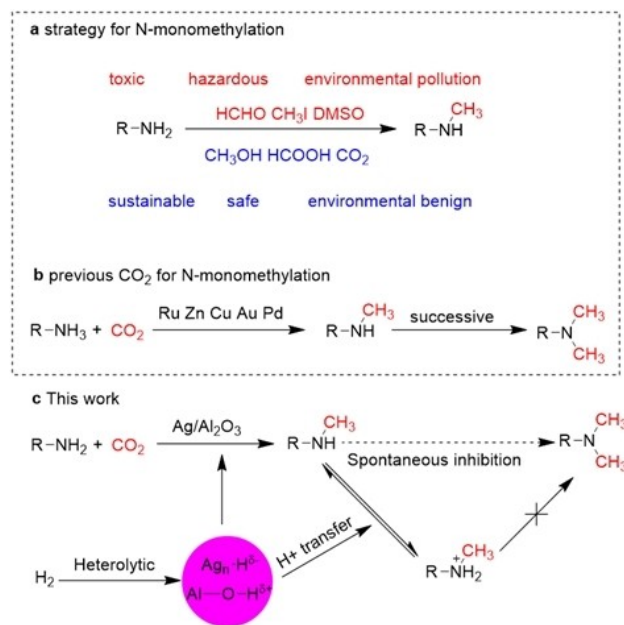
Supporting information for this article is available on the WWW under <https://doi.org/10.1002/chem.202203152>

© 2023 The Authors. Chemistry - A European Journal published by Wiley-VCH GmbH. This is an open access article under the terms of the Creative Commons Attribution Non-Commercial License, which permits use, distribution and reproduction in any medium, provided the original work is properly cited and is not used for commercial purposes.

neous and heterogeneous catalysts have been reported for the methylation of amines with CO₂ by using silane, borane or H₂ as reductants. Compared to homogenous catalysts, heterogeneous catalytic systems have more industrialization potential due to easy separation and reusability of the catalysts and are thus more desirable. Although many heterogeneous catalysts such as Au/A₂O₃,^[18] Re/TiO₂,^[19] N-doped porous carbons (NPCs)^[16b] and PdZn/TiO₂^[20] have been reported as good catalysts for the synthesis of tertiary amines, they do not perform well for the synthesis of monomethylated amines, due to the aforementioned thermodynamic advantage of tertiary amines. Shi and collaborators first reported that CuAlOx and PdCuZrOx could be used as catalysts for the synthesis of monomethylated amines.^[21] Tamura's group reported that the sub-nanoparticles of Cu supported on CeO₂ can catalyze the N-methylation of aniline with CO₂/H₂, and a selectivity of *N*-methylaniline of over 90% was obtained at optimal reaction conditions.^[22] Although the above-mentioned strategies can generate *N*-monomethylamines with high selectivity by controlling multiple reaction conditions, they mostly suffer from a relatively low yield of the target products (i.e. the conversion of aniline in Tamura's report does not exceed 70%, while a more detailed comparison is listed in Supporting Information, Table S1). Therefore, the development of more concise, direct, and efficient strategies for the selective synthesis of *N*-monomethylated amines is highly appealing. In this study, we try to design a catalyst which can reduce the reactivity of secondary amines and thus prevent over methylation in a wide variety of amines.

Supported Ag-based catalysts are widely used for selective oxidation of NH₃,^[23] alcohols^[24] and olefins,^[25] formaldehyde purification,^[26] and hydrogenation of CO₂.^[27] Despite these examples, methods for amines reacting with CO₂ to form monomethylated amines via Ag catalysts have not previously been reported. Intriguingly, supported Ag catalysts have been used for heterolytic dissociation of hydrogen^[28] and selective synthesis of secondary amines from aniline.^[29] Furthermore, H⁺ reacts with amine to form ammonium salts, which can limit the binding of the amine nitrogen to metals and hence reducing its reactivity.^[30] As such, we envision that H⁺ from the heterolytic dissociation of H₂ on Ag catalyst is prompt to combine with the stronger alkaline *N*-methyl amine, reducing the reactivity of *N*-monomethylamines and thus inhibiting the formation of tertiary amines (Scheme 1).

Herein, we report a new strategy by employing for the first time a supported Ag/Al₂O₃ catalyst for the selective synthesis of *N*-monomethylated amines by using CO₂/H₂ as C1 source. The catalyst can heterolytically dissociate H₂, enabling the synthesis of monomethylated amines with high selectivity due to spontaneous inhibition of over-methylation processes. In this way, various *N*-monomethylated amines were obtained with high selectivity and yield from their corresponding primary amines, using the sustainable route of CO₂/H₂ as primary reagents. Our findings give a new insight for designing efficient catalysts towards the sustainable synthesis of *N*-monomethylated amines.



Scheme 1. a. Strategy for selective *N*-monomethylation. b. Previously reported ideas on CO₂ utilization in the *N*-methylation of amines. c. Our proposal in this work for selective *N*-monomethylation of amines.

Results and Discussion

We first carried out density functional theory (DFT) calculations to understand the effect of Ag catalyst on the selectivity of *N*-methylation products. Because of the complexity of the interfacial structure between the Ag metal and Al₂O₃, we simplified the interface model of Ag (111)/Al₂O₃ like in a previous report^[31] and evaluated the dissociation energy of H₂. As shown in Figure 1a, the calculated reaction energy for H₂ heterolytic dissociation on Al–O–Ag was not more stable but

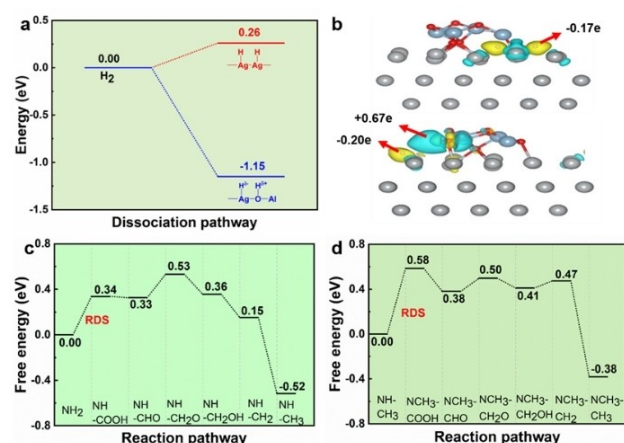


Figure 1. a. The dissociation of H₂ on the surfaces of Al₂O₃/Ag (111). b. The charge distribution of H from homolytic dissociation and heterolytic dissociation on Ag (111). c. Energy profiles for CO₂/H₂ with aniline forming *N*-methylaniline on Ag (111). d. CO₂/H₂ with *N*-methylaniline forming *N,N*-dimethylaniline on Ag (111).

lower than that of the homolytic dissociation on Ag–Ag (−1.15 eV vs. 0.26 eV), which means that the H₂ dissociation occurred via the heterolytic route on the interface of Ag and Al₂O₃. The charge distribution (Figure 1b) shows that the charge of the H resulted from the homolytic dissociation was −0.17e, while the Ag–H^{δ−} and Al–O–H^{δ+} from the heterolytic dissociation were −0.2e and +0.67e, respectively. These results indicate that the heterolytic dissociation of H₂ leads to the generation of protonated H. Generally, the protonated H will react with the methylated amines, in situ, to form ammonium salts due to methylated amines having a stronger alkalinity, thus reducing the reactivity of N-methylamines.

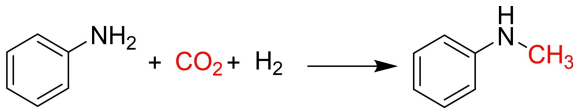
Next, the reaction pathways of aniline N-methylation reported previously in the literature were evaluated.^[22] The adsorbed aniline could produce phenylcarbamic acid via N–H breaking and react with *COOH. The phenylcarbamic acid sequentially combines with H dissociated from H₂ on the surface of the catalyst to generate the N-methylated product through double dehydration. Similarly, the N-monomethylaniline follows the same steps to get the N,N-dimethylated product. We found that the formation of N-COOH is the rate-determining step for both the aniline to N-monomethylaniline and from N-monomethylaniline to the N-dimethylaniline (as shown in Figure 1c and 1d). However, the formation energy of NH–COOH (0.34 eV) is much lower than that of CH₃N–COOH (0.58 eV), indicating that the methylation of the secondary amine is more difficult (Figure 1d). These results highlight the selective monomethylation of amines on Ag (111) based on the difference in energy barriers of the rate-determining steps for methylation between primary and secondary amines.

To verify our prediction, a series of Ag based catalysts were prepared by the incipient wetness method and tested for monomethylation of aniline with CO₂/H₂. A yield of over 90% of the monomethylated product was obtained under optimal reaction conditions. Control experiments demonstrate that N-methylaniline was unlikely to further methylate over the Ag/Al₂O₃ catalyst.

To extract the target N-methylaniline, the influence of solvent was first investigated (Table 1, entries 1–6). When tetrahydrofuran (THF) was employed, only 20% selectivity of N-methylaniline (with 20% conversion of aniline) could be obtained, while the remaining 80% of the product was N-phenylpyrrolidine, meaning the THF reacted with aniline. When the temperature was increased up to 200 °C and cyclohexane was used as solvent, a 31% conversion of aniline with excellent selectivity (>99%) of the target product was achieved. Hexadecane, on the other hand, showed no reaction activity. Although the conversion of aniline can be increased with other solvents, including dodecane and hexane, the selectivity of N-methylaniline decreases sharply. Thus, the cyclohexane solvent provided the best traded off for this reaction (i.e. in the balance of reactivity and selectivity).

Following, a Ag catalyst on different supports (SiO₂, TiO₂) was tested (Table 1, entries 7, 8). Obviously, Ag/Al₂O₃ exhibits the best catalytic performance with 31% conversion and >99% selectivity. Ag/TiO₂ delivered a 20% conversion of aniline with a 99% selectivity of N-methylaniline, while Ag/SiO₂ showed no

Table 1. N-monomethylation of aniline with CO₂/H₂ over various catalysts.^[a]



Entry	Catalyst	Solvent	T [°C]	Conv. [%]	Select. [%]
1	5% Ag/Al ₂ O ₃	THF	180	20	20
2	5% Ag/Al ₂ O ₃	Cyclohexane	200	31	> 99
3	5% Ag/Al ₂ O ₃	Octane	200	28	72
4	5% Ag/Al ₂ O ₃	Dodecane	200	36	74
5	5% Ag/Al ₂ O ₃	Hexadecane	200	N.R.	
6	5% Ag/Al ₂ O ₃	Hexane	200	41	69
7	5% Ag/SiO ₂	Cyclohexane	200	N.R.	
8	5% Ag/TiO ₂	Cyclohexane	200	21	99
9	Al ₂ O ₃	Cyclohexane	200	N.R.	
10	2% Ag/Al ₂ O ₃	Cyclohexane	200	5.7	> 99
11	10% Ag/Al ₂ O ₃	Cyclohexane	200	66	97
12	20% Ag/Al ₂ O ₃	Cyclohexane	200	67	97
13	10% Ag/Al ₂ O ₃	Cyclohexane	230	83	96
14	10% Ag/Al ₂ O ₃	Cyclohexane	250	100	84

Reaction conditions: aniline 0.18 g (2 mmol), CO₂ 3 MPa, H₂ 3 MPa, catalyst 50 mg, solvent 5 ml, 10 h. [a] Detected by GC-MS.

activity. Indeed, Al₂O₃ has suitable acidic and basic sites and interacts strongly with Ag,^[29b,32] resulting in a superior performance of the Ag nanoparticles when employing this support. In comparison, other metals supported on Al₂O₃ were also tested. The results are listed in Table S2. Among them, Fe, Co, Ni, Cu, Zn had no activity, while the main product of noble metals Ru, Rh, Pd was diphenylamine, meaning that a deamination reaction occurred.

To optimize the catalyst loading, different concentrations were investigated (Table 1 entry 9–14). A detailed distribution of the products is shown in Table S3. The pristine Al₂O₃ had no reaction activity. For Ag/Al₂O₃, the conversion of aniline increased from 5.7 to 66% with Ag loadings varying from 2% to 10%, respectively. The selectivity of N-methylaniline was higher than 95% for all the Ag/Al₂O₃ samples. Further increase in the Ag loading up to 20% did not lead to any significant change compared to 10% Ag/Al₂O₃, indicating that the suitable loading is around 10% Ag/Al₂O₃.

When the reaction temperature increased from 200 °C to 230 °C, the conversion of aniline also increased from 66% to 83% and the selectivity of N-methylaniline was 96%. Although the complete conversion of aniline could be obtained by further increasing the temperature to 250 °C, the selectivity of N-methylaniline dropped to 84%. Thus, a reaction temperature of 230 °C is the optimal one to maintain the highest yield/selectivity ratio for N-methylaniline.

In order to determine the most suitable reaction time, the product distribution study for the 10% Ag/Al₂O₃ catalyst was performed. As shown in Figure 2, the conversion of aniline increases with the reaction time. When the reaction time reached 24 h, 100% conversion of aniline with 90.4% selectivity of N-methylaniline was achieved. Further extending the reaction time to 36 h led to a slight decrease in the selectivity of N-methylaniline to 88.8%, which indicates that best reaction time was 24 h, meanwhile, extending reaction time only slightly

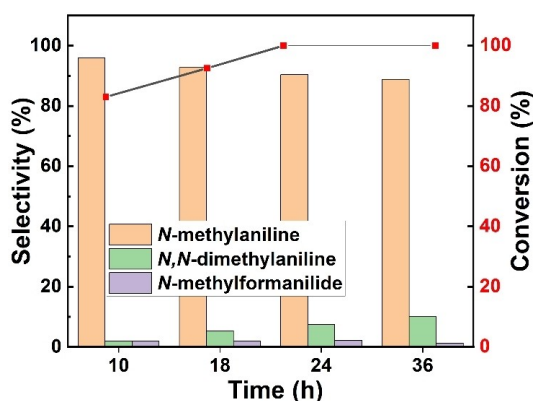


Figure 2. Products distribution under optimized conditions with different reaction times. Reaction conditions: amines 2 mmol, CO₂ 3 MPa, H₂ 3 MPa, catalyst 50 mg, cyclohexane 5 mL, 230 °C.

decreases the selectivity of target product indicate the catalyst can efficiently inhibit the methylation of *N*-methylaniline to tertiary amines. These results are in agreement with the DFT calculations shown in Figure 1. Although the selectivity of *N*-methylaniline remained above 90%, the catalyst was obviously deactivated during reuse. Therefore, we raised the reaction temperature to 230 °C and extended the reaction time, which significantly improved the conversion of aniline while maintaining a high selectivity of *N*-methylaniline. (Figure S2-1 and S2-2).

To verify the catalytic behaviour of the Ag/Al₂O₃ catalyst, *N*-methylaniline was employed as reactant to replace aniline (Scheme S1). Under the same condition, only a 27% conversion of *N*-methylaniline, with a 67% selectivity for *N*, *N*-dimethylaniline was obtained after 24 h. Compared with the 100% conversion yield of aniline and 90.4% selectivity for the monomethylated product, both the conversion yield of *N*-methylaniline and selectivity of target product decreased significantly, even the reactivity of *N*-methylaniline is much higher than that of aniline. These results demonstrated that the synthesis of *N*-methylaniline can be achieved by suppressing the successive methylation on Ag/Al₂O₃.

To understand the structure-activity relationship of the catalysts, comprehensive characterization experiments were conducted. Inductively coupled plasma optical emission spectrometer (ICP-OES) showed that the Ag loading in the different samples were very close to their theoretical values (Table S4). The Ag on the catalyst is gradually leached with recycling test, which should be the reason for the deactivation of catalyst during recycling, but the decrease of Ag content in the solvent means that the loss of Ag is slowed down in the subsequent test. Based on the Brunauer–Emmett–Teller (BET) isotherm results (Table S5), with the increase of Ag loading from 0% to 20%, the specific surface areas and the pore volumes decrease from 118 m²/g to 95 m²/g and 0.755 cm³/g to 0.578 cm³/g, respectively. The diameter does not change significantly (from 2.56 nm to 2.38 nm), indicating that the Ag species were mainly dispersed on the surface of Al₂O₃.

X-ray photoelectron spectroscopy (XPS) spectra of the 10% Ag/Al₂O₃ (Figure 3a) results show that Ag 3d_{5/2} and 3d_{3/2} signal appeared at 368.1 eV and 374.1 eV respectively, which suggested that metallic Ag was mainly formed on the surface of catalyst.^[33] From the X-ray diffraction (XRD) patterns (Figure 3b), the crystalline phase of Ag becomes apparent with the increasing Ag loadings. The 10% Ag/Al₂O₃ sample shows the Ag (111) and Ag (100) facets, which is in agreement with the XPS results. Ag K-edge X-Ray absorption fine structure (EXAFS) was applied for revealing the coordination environment of Ag in the Ag/Al₂O₃ (Figure S4). The fitting results are summarized in the Table S6. From the results, we can determine that the coordination number of Ag–Ag were mainly from 3.9 to 4.7, which is larger than that of Ag–O (~1). This results also indicates that metallic Ag is dominant in samples.

Transmission Electron Microscope (TEM) was employed to further characterize the morphology and crystal facet of the 10% Ag/Al₂O₃ catalyst. As shown in Figure 4, lattice fringes can be clearly discerned with *d*-spacing of 0.24 and 0.21 nm, which could be assigned to the Ag (111) and Ag (100) planes. High-angle annular dark field scanning TEM further demonstrate this results. Both the obtained results and the XRD results means

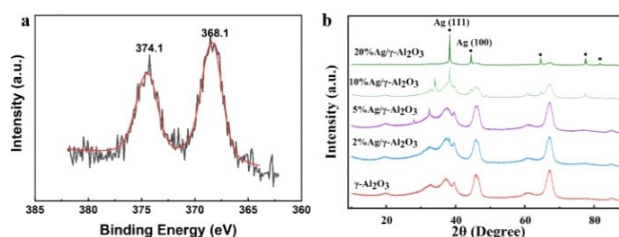


Figure 3. a. XPS image for Ag 3d of the 10% Ag/Al₂O₃. b. XRD patterns of the Ag/Al₂O₃ catalyst with 0%, 2%, 5%, 10% and 20% Ag loadings.

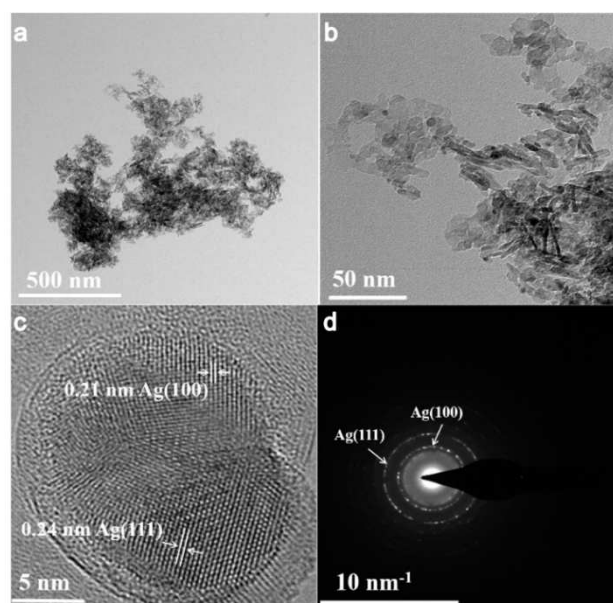


Figure 4. TEM (a, b), HRTEM (c), and HAADF (d) images of 10% Ag/Al₂O₃.

that the Ag (111) and Ag (100) were the main crystal planes. Energy dispersive X-ray spectroscopy (EDX) maps (Figure S3) show that the Ag nanoparticles are well dispersed on Al₂O₃ support (not large than 25 nm). The catalyst was also tested after being used for 5 rounds (Figure S5). The nanoparticles were aggregation (even larger than 50 nm) in the catalyst after five times used compared to the fresh catalyst, which should be one of the reason for activity decreased of catalyst.

In order to examine the reaction process of aniline with CO₂/H₂ to synthesize *N*-methylaniline, in situ diffuse reflectance Fourier transform infrared spectroscopy (in situ DRIFTS) spectra were acquired (Figure 5). At the beginning of the reaction, no absorption bands could be observed on the catalyst. After 5 min from the start of the reaction, an absorption band appeared at 1590 cm⁻¹, which can be assigned to *COOH species.^[34] The signal intensity increased over time. However, there were no obvious changes from min 10 to min 30 of the reaction, suggesting that the *COOH was the main product formed on the catalyst. Moreover, a second absorption band at 2905 cm⁻¹ can be assigned to C–H vibrations, indicating the dissociated H combine with *COOH. This proves that *COOH was the key intermediate formed from CO₂ and H₂ over the catalyst.

To further prove the heterolytic dissociation of H₂ can reduce the reactivity of secondary amines, the in situ DRIFTS of *N*-methylaniline was carried out under reaction conditions. As the Figure S6 shows, the spectral lines are typical for *N*-methylaniline. A broad band occur at 3412 cm⁻¹ means that *N*-methylaniline bind with H⁺ and formed Ammonium salt. Other two peaks at 1315 cm⁻¹ and 1504 cm⁻¹ can be attributed C–N and C–H stretching respectively.^[35] In addition, the signal intensity first rise then falls indicating that the reaction process is reversible. This result demonstrated that the H⁺ from heterolytic can indeed reduce the reactivity of *N*-methylaniline, which is consistent with our prediction and DFT results.

According to the in situ DRIFTS results and our calculations, a possible reaction mechanism is proposed (Scheme 2). Firstly, *COOH species are generated from CO₂ and H₂. Then, phenyl-carbamic acid is obtained from aniline that reacts with the *COOH and subsequently dehydrate to formanilide, which is further dehydration to get the target *N*-methylaniline. *N*-methylation of aniline with CO₂/H₂ under 180 °C with different times demonstrate that the formanilide is an intermediate in the reaction, as its content decreased with the extension of reaction

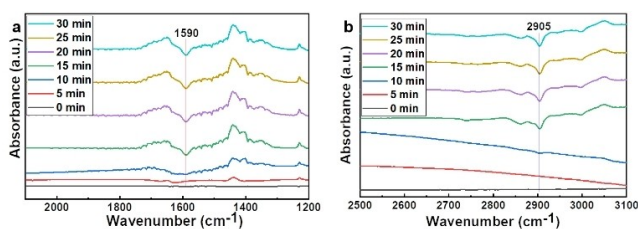
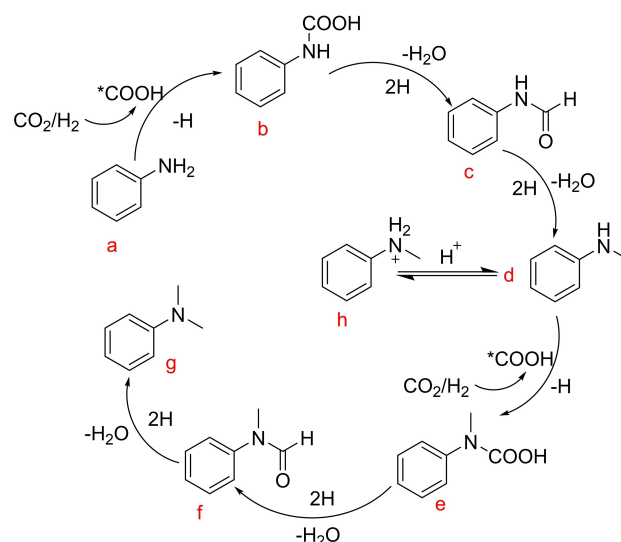


Figure 5. In-situ DRIFTS spectra of 10% Ag/Al₂O₃ exposure to CO₂ (0.3 MPa) and H₂ (0.3 MPa) at 230 °C with different reaction times. a. low wavenumber. b. High wavenumber.

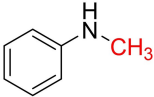
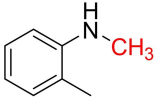
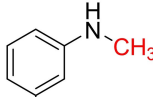
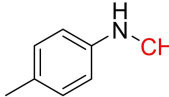
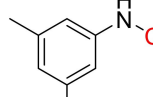
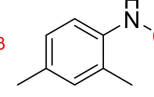
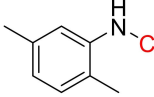
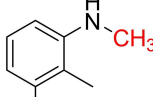
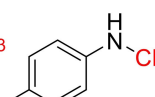
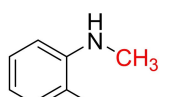
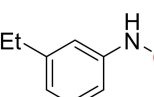
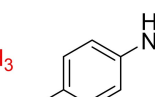
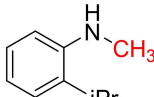
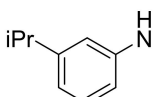
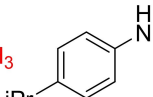
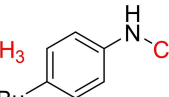
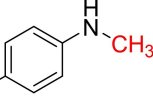
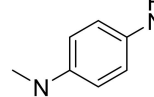
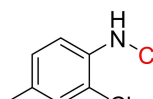
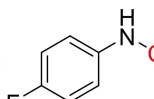
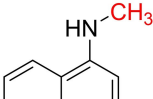


Scheme 2. The reaction process for the *N*-methylation of aniline with CO₂ and H₂.

time. This reaction mechanism agrees well with our DFT calculations. According previous reports, the heterolysis of H₂ on Ag and Al₂O₃ interface to generate H⁺ can combine/decompose with monomethylated amines and reduce its reactivity, making it difficult to further methylate and form tertiary amines.

Finally, under the optimal reaction conditions, the general applicability of the *N*-monomethylation protocol was investigated. As shown in Table 2, when aniline contains alkyl electron-donating groups such as –CH₃, ethyl (Et), isopropyl (*i*-Pr), *n*-butyl (*n*-Bu), *t*-butyl (*t*-Bu) (Table 2, 3b–3r), good to excellent yields (60%–98%) can be obtained for the corresponding monomethylated products. Among them, the 4-*N*-butyl-aniline led to the highest yield of monomethylated product (98%). The ortho-substitution shows a lower reaction efficiency than their para or meta substituted analogues (Table 2, 3b, 3f, 3h, 3j, 3m), which is assigned to a steric hindrance effects. When the 2-chloro-4-methylaniline (Table 2, 3s) and 4-fluoroaniline (Table 2, 3t) are used as substrates, the yield of monomethylated products decreased significantly (51% and 49%, respectively), indicating that the *N*-monomethylation of amines is a typical nucleophilic feature. In addition, we have detected that hydrodehalogenation has occurred, which should also be the reason for the low yield. Naphthylamine forms its monomethylated product with a yield of 57% (Table 2, 3u). These results demonstrate that the Ag/Al₂O₃ catalyst has a good tolerance to different substrates. Although relative high yields were obtained when alkyl substituted aromatic amines were used as substrates, the catalytic system does not adopt to a wide range of substrates due to harsh reaction conditions. When we test other anilines substituted by different functional groups, violent hydrogenolysis reaction will result in very low yield of the target product.

Table 2. N-monomethylation of amines with CO₂/H₂ catalysis by 10% Ag/Al₂O₃.^[a]

1		2		3	
$\text{R-NH}_2 + \text{CO}_2 + \text{H}_2 \xrightarrow[\text{Cyclohexane, 230}^\circ\text{C, 24h}]{0.046 \text{ mmol } 10\% \text{ Ag/Al}_2\text{O}_3} \text{R-N(CH}_3\text{)}_2$					
					
3a 90% (85%) ^b	3b 67% (63%) ^b	3c 82% (80%) ^b	3d 83% (77%) ^b	3e 85%	3f 68%
					
3g 73%	3h 63%	3i 80%	3j 60%	3k 77%	3l 76%
					
3m 61%	3n 83%	3o 80%	3p 88%	3q 98%	3r 66%
					
3s 51%	3t 49% (42%) ^b	3u 57% (54%) ^b			

Reaction conditions: amines 2 mmol, CO₂ 3 MPa, H₂ 3 MPa, catalyst 50 mg (0.046 mmol Ag), cyclohexane 5 mL, 230 °C, 24 h. [a] The yields were determined by GC using biphenyl as internal standard. [b] Isolated yield.

Conclusion

We show for the first example that a Ag/Al₂O₃ catalyst can selective synthesis of N-monomethylated amines by using CO₂/H₂ as C1 source. The protonated hydrogen produced by the heterolytic dissociation of hydrogen over the Ag catalyst could bind reversibly to N-monomethylated amines, strongly reducing their reactivity. DFT calculations show that the rate determining energy barrier of primary amines methylation over the Ag (111) catalyst's surface is 0.34 eV, which is much lower than that of secondary amines over the same catalyst (0.58 eV). This prevents multiple methylation cycles, turning the catalyst into a highly selective route for N-monomethylated amines. The experimental results presented in this study further support our theoretical predictions. BET, EXAFS, XRD, XPS, HADDF-STEM results show that the Ag species consist mainly in nanoparticles on Al₂O₃, and that Ag (111) is the main exposed facet. In-situ DRIFTS revealed that *COOH are intermediates of the reaction on this catalyst, and prove the heterolytic dissociation of H₂ can reduce the reactivity of secondary amines. A probable reaction mechanism has been proposed based on these results. In

summary, we present a novel, efficient and straightforward method for the synthesis of N-monomethylated amines following a sustainable route.

Experimental Section

The Ag/Al₂O₃ catalyst were prepared by the incipient wetness method using Ag(NO₃)₃ (Sinopharm Chemical Reagent Co., Ltd, China) as precursor. The Al₂O₃ support (20 nm), supplied by the Shanghai Aladdin Biochemical Technology Co. Ltd., was dried at 110 °C for 12 h prior to use. After impregnation of the aqueous solutions of the precursors with a certain concentration, the sample was dried at 80 °C for 12 h, then calcined at 400 °C for 3 h, and reduced under a hydrogen flow at 300 °C for 5 h. The catalysts with different weight loadings of Ag were denoted x% Ag/Al₂O₃. Other catalysts were prepared via the same method. The detail characterization methods were listed in Supporting Information.

Catalytic reactions were carried out in a 25 ml stainless steel autoclave with a magnetic stirrer. In a typical process, aniline (2 mmol), catalyst (50 mg) and 5 ml solvent were charged in the autoclave. The autoclave was sealed and purged three times with CO₂ gas, then pressurized to 3 MPa with CO₂, and finally charged

with 3 MPa of H₂ gas. The total pressure of the autoclave was found to be around 6 MPa. The reactor was heated to 230 °C and magnetically stirred constantly during the reaction. After reaction, the qualitative and quantitative analyses of the resulting liquid mixture were analyzed by the Shimadzu GCMS-QP 2020 NX equipped with a 30 m Rtx-5 MS fused silica column (i.d.0.25 mm; 0.25 μm film thickness) and Shimadzu GC (Shimadzu 2010) equipped with a SE-54 capillary column and a FID detector. The products were isolated by silica column separation.

The used catalyst was separated from the reaction mixture by centrifuging, followed by washing the catalyst three times with cyclohexane. After being dried in air at 110 °C for 4 h, it was recovered and directly recharged into the reaction autoclave for the next run.

Density functional theory (DFT) calculations were performed with the PBE exchange-correlation functional and the projector augmented wave (PAW) method with the Vienna ab initio simulation package (VASP). The energy cutoff of plane wave was set to 400 eV. The convergence criteria for the iteration process were set to less than 0.02 eV·Å⁻¹ for the maximal residual force and to less than 10⁻⁵ eV for the energy change. A Monkhorst-Pack mesh with 2 × 2 × 1 K-points was used for the Brillouin zone integration. To understand the reaction mechanism on Ag surface, we build a (4 × 4 × 3) Ag supercell slab containing 48 Ag atoms. Vacuum layer is set to 15 Å. The Gibbs free energy of each elementary step was calculated as

$$\Delta G = \Delta E + \Delta ZPE - T \cdot \Delta S$$

where ΔE is the reaction energy calculated by the DFT method. ΔZPE and ΔS are the changes in the zero-point energies and entropy during the reaction, respectively.

Acknowledgements

We thank the Natural Science Foundation of China (Grant No. 21872174, 22002189, and U1932148), International Science and Technology Cooperation Program (Grant No. 2017YFE0127800 and 2018YFE0203402), Hunan Province Key Field R&D Program (2020WK2002), Hunan Provincial Natural Science Foundation (2020JJ2041 and 2020JJ5691), Shenzhen Science and Technology Innovation Project (Grant No. J-CYJ20180307151313532). We also acknowledge funding and support from the Deutsche Forschungsgemeinschaft (DFG, German Research Foundation) under Germany's Excellence Strategy – EXC 2089/1 – 390776260, the Bavarian Program Solar Energies Go Hybrid (SolTech), the Center for NanoScience (CeNS) and the European Commission through the ERC Starting Grant CATALIGHT (802989). We are grateful for resources from the High Performance Computing Center of Central South University. Open Access funding enabled and organized by Projekt DEAL.

Conflict of Interest

The authors declare no conflict of interest.

Data Availability Statement

The data that support the findings of this study are available from the corresponding author upon reasonable request.

Keywords: Al₂O₃ · CO₂ utilization · heterogeneous catalysis · monomethylation of amines · silver

- [1] E. S. Sanz-Pérez, C. R. Murdock, S. A. Didas, C. W. Jones, *Chem. Rev.* **2016**, *116*, 11840–11876.
- [2] a) J. Artz, T. E. Müller, K. Thenert, J. Kleinekorte, R. Meys, A. Sternberg, A. Bardow, W. Leitner, *Chem. Rev.* **2018**, *118*, 434–504; b) M. D. Burkart, N. Hazari, C. L. Tway, E. L. Zeitler, *ACS Catal.* **2019**, *9*, 7937–7956; c) S. Dabral, T. Schaub, *Adv. Synth. Catal.* **2019**, *361*, 223–246.
- [3] a) M. Liu, Y. Pang, B. Zhang, P. De Luna, O. Voznyy, J. Xu, X. Zheng, C. T. Dinh, F. Fan, C. Cao, *Nature* **2016**, *537*, 382–386; b) K. Chen, M. Cao, Y. Lin, J. Fu, H. Liao, Y. Zhou, H. Li, X. Qiu, J. Hu, X. Zheng, *Adv. Funct. Mater.* **2022**, *32*, 2111322; c) A. Laemont, S. Abednatanzi, P. G. Derakshandeh, F. Verbruggen, E. Fiset, Q. Qin, K. Van Daele, M. Meledina, J. Schmidt, M. Oschatz, *Green Chem.* **2020**, *22*, 3095–3103.
- [4] a) W. Ma, S. Xie, X.-G. Zhang, F. Sun, J. Kang, Z. Jiang, Q. Zhang, D.-Y. Wu, Y. Wang, *Nat. Commun.* **2019**, *10*, 892; b) K. Schlenker, E. G. Christensen, A. A. Zhanerkeev, G. R. McDonald, E. L. Yang, K. T. Lutz, R. P. Steele, R. T. VanderLinden, C. T. Saouma, *ACS Catal.* **2021**, *11*, 8358–8369.
- [5] a) Y.-Y. Liu, H.-L. Zhu, Z.-H. Zhao, N.-Y. Huang, P.-Q. Liao, X.-M. Chen, *ACS Catal.* **2022**, *12*, 2749–2755; b) J. Fu, K. Liu, K. Jiang, H. Li, P. An, W. Li, N. Zhang, H. Li, X. Xu, H. Zhou, *Adv. Sci.* **2019**, *6*, 1900796.
- [6] J. Zhu, F. Cannizzaro, L. Liu, H. Zhang, N. Kosinov, I. A. Filot, J. Rabeah, A. Brückner, E. J. Hensen, *ACS Catal.* **2021**, *11*, 11371–11384.
- [7] P. Gao, S. Li, X. Bu, S. Dang, Z. Liu, H. Wang, L. Zhong, M. Qiu, C. Yang, J. Cai, *Nat. Chem.* **2017**, *9*, 1019–1024.
- [8] Q. Liu, L. P. Wu, R. Jackstell, M. Beller, *Nat. Commun.* **2015**, *6*, 5933.
- [9] Y. H. Li, X. J. Cui, K. W. Dong, K. Junge, M. Beller, *ACS Catal.* **2017**, *7*, 1077–1086.
- [10] a) M. Onaka, K. Ishikawa, Y. Izumi, *Chem. Lett.* **1982**, *11*, 1783–1786; b) R. N. Salvatore, C. H. Yoon, K. W. Jung, *Tetrahedron* **2001**, *57*, 7785–7812.
- [11] H. Wang, H. Yuan, B. Yang, X. Dai, S. Xu, F. Shi, *ACS Catal.* **2018**, *8*, 3943–3949.
- [12] X. Jiang, C. Wang, Y. Wei, D. Xue, Z. Liu, J. Xiao, *Chem. Eur. J.* **2014**, *20*, 58–63.
- [13] a) O. Ogata, H. Nara, M. Fujiwhara, K. Matsumura, Y. Kayaki, *Org. Lett.* **2018**, *20*, 3866–3870; b) G. Choi, S. H. Hong, *Angew. Chem. Int. Ed. Engl.* **2018**, *57*, 6166–6170; c) S. Elangovan, J. Neumann, J. B. Sortais, K. Junge, C. Darcel, M. Beller, *Nat. Commun.* **2016**, *7*, 12641; d) T. T. Dang, B. Ramalingam, A. M. Seayad, *ACS Catal.* **2015**, *5*, 4082–4088.
- [14] a) I. Sorribes, K. Junge, M. Beller, *Chem. Eur. J.* **2014**, *20*, 7878–7883; b) S. Savourey, G. Lefèvre, J.-C. Berthet, T. Cantat, *Chem. Commun.* **2014**, *50*, 14033–14036.
- [15] a) A. Dhakshinamoorthy, M. Alvaro, H. Garcia, *Appl. Catal. A* **2010**, *378*, 19–25; b) R. Juarez, A. Padilla, A. Corma, H. Garcia, *Catal. Commun.* **2009**, *10*, 472–476.
- [16] a) A. Gopakumar, L. Lombardo, Z. Fei, S. Shyshkanov, D. Vasilyev, A. Chidambaram, K. Stylianou, A. Zuttel, P. J. Dyson, *J. CO₂ Util.* **2020**, *41*, 101240; b) F. Tang, L. Wang, Y.-N. Liu, *Green Chem.* **2019**, *21*, 6252–6257; c) K. Beydoun, G. Ghattas, K. Thenert, J. Klankermayer, W. Leitner, *Angew. Chem. Int. Ed.* **2014**, *126*, 11190–11194; d) Y. Li, I. Sorribes, T. Yan, K. Junge, M. Beller, *Angew. Chem. Int. Ed.* **2013**, *52*, 12156–12160; *Angew. Chem.* **2013**, *125*, 12378–12382; e) Y. Li, X. Fang, K. Junge, M. Beller, *Angew. Chem. Int. Ed.* **2013**, *52*, 9568–9571; *Angew. Chem.* **2013**, *125*, 9747–9750; f) O. Jacquet, X. Frogneux, C. Das Neves Gomes, T. Cantat, *Chem. Sci.* **2013**, *4*, 2127–2131.
- [17] J. Wang, J. Wu, Z.-N. Chen, D. Wen, J. Chen, Q. Zheng, X. Xu, T. Tu, J. Catal. **2020**, *389*, 337–344.
- [18] X.-L. Du, G. Tang, H.-L. Bao, Z. Jiang, X.-H. Zhong, D. S. Su, J.-Q. Wang, *ChemSusChem* **2015**, *8*, 3489–3496.
- [19] T. Toyao, S. H. Siddiki, Y. Morita, T. Kamachi, A. S. Touchy, W. Onodera, K. Kon, S. Furukawa, H. Ariga, K. Asakura, *Chem. Eur. J.* **2017**, *23*, 14848–14859.
- [20] W. Lin, H. Cheng, Q. Wu, C. Zhang, M. Arai, F. Zhao, *ACS Catal.* **2020**, *10*, 3285–3296.

- [21] a) X. Cui, X. Dai, Y. Zhang, Y. Deng, F. Shi, *Chem. Sci.* **2014**, *5*, 649–655; b) X. Cui, Y. Zhang, Y. Deng, F. Shi, *Chem. Commun. (Camb.)* **2014**, *50*, 13521–13524.
- [22] M. Tamura, A. Miura, Y. Gu, Y. Nakagawa, K. Tomishige, *Chem. Lett.* **2017**, *46*, 1243–1246.
- [23] Z. Qu, H. Wang, S. Wang, H. Cheng, Y. Qin, Z. Wang, *Appl. Surf. Sci.* **2014**, *316*, 373–379.
- [24] V. V. Torbina, A. A. Vodyankin, S. Ten, G. V. Mamontov, M. A. Salaev, V. I. Sobolev, O. V. Vodyankina, *Catalysts* **2018**, *8*, 447.
- [25] A. Chongterdtoonskul, J. W. Schwank, S. Chavadej, *J. Mol. Catal. A* **2012**, *358*, 58–66.
- [26] X. Chen, M. Chen, G. He, F. Wang, G. Xu, Y. Li, C. Zhang, H. He, *J. Phys. Chem. C* **2018**, *122*, 27331–27339.
- [27] J. J. Corral-Pérez, C. Copéret, A. Urakawa, *J. Catal.* **2019**, *380*, 153–160.
- [28] a) T. Baba, N. Komatsu, H. Sawada, Y. Yamaguchi, T. Takahashi, H. Sugisawa, Y. Ono, *Langmuir* **1999**, *15*, 7894–7896; b) T. Baba, H. Sawada, T. Takahashi, M. Abe, *Appl. Catal. A* **2002**, *231*, 55–63; c) T. Baba, Y. Tohjo, T. Takahashi, H. Sawada, Y. Ono, *Catal. Today* **2001**, *66*, 81–89.
- [29] a) H. Liu, G.-K. Chuah, S. Jaenicke, *J. Catal.* **2012**, *292*, 130–137; b) K. Shimizu, M. Nishimura, A. Satsuma, *ChemCatChem* **2009**, *1*, 497–503.
- [30] M. Lee, M. S. Sanford, *J. Am. Chem. Soc.* **2015**, *137*, 12796–12799.
- [31] C. Xu, G. Chen, Y. Zhao, P. Liu, X. Duan, L. Gu, G. Fu, Y. Yuan, N. Zheng, *Nat. Commun.* **2018**, *9*, 3367.
- [32] F. Wang, J. Ma, S. Xin, Q. Wang, J. Xu, C. Zhang, H. He, X. Cheng Zeng, *Nat. Commun.* **2020**, *11*, 529.
- [33] H. Kannisto, H. H. Ingelsten, M. Skoglundh, *J. Mol. Catal. A* **2009**, *302*, 86–96.
- [34] X. Li, Y. Sun, J. Xu, Y. Shao, J. Wu, X. Xu, Y. Pan, H. Ju, J. Zhu, Y. Xie, *Nat. Energy* **2019**, *4*, 690–699.
- [35] M. Navaneethan, K. Nisha, S. Ponnusamy, C. Muthamizhchelvan, *Rev. Adv. Mater. Sci* **2009**, *21*, 217–224.

Manuscript received: October 10, 2022

Accepted manuscript online: January 10, 2023

Version of record online: March 1, 2023